Fate of topological states in incommensurate generalized Aubry-André models

J. C. C. Cestari, A. Foerster, and M. A. Gusmão
Universidade Federal do Rio Grande do Sul, C.P. 15051, 91501-970 Porto Alegre, Brazil
(Received 14 January 2016; revised manuscript received 4 April 2016; published 31 May 2016)

We study one-dimensional optical lattices described by generalized Aubry-André models that include both commensurate and incommensurate modulations of the hopping amplitude. This brings together two interesting features of this class of systems: Anderson localization and the existence of topological edge states. We follow changes of the single-particle energy spectrum induced by variations of the system parameters, with focus on the survival of topological states in the localized regime.

DOI: 10.1103/PhysRevB.93.205441

I. INTRODUCTION

In recent years, rapid progress in techniques for creating ultracold-atom systems in the laboratory allowed the experimental realization of many interesting models originally proposed to study specific properties of real solids. For instance, the construction of bichromatic lattices with incommensurate potentials led to observation [1–3] of the Anderson-localization transition [4] in one dimension, which cannot happen for true disorder. Such a transition has received the attention of theoreticians for many years [5–10]. In this context, the standard theoretical approach utilizes the Aubry-André (AA) model [11], intimately related to the Harper-Hofstadter (HH) model [12,13] for electrons in a two-dimensional (2D) lattice in the presence of a perpendicular magnetic field. The latter is mapped onto a one-dimensional (1D) system with a modulating potential superimposed to the lattice, its period $(1/\beta)$ being determined by the magnetic-field intensity. Thus, the relative periodicities between modulating potential and lattice can be tuned in principle to any ratio. The energy spectrum for varying β appears as the famous Hofstadter butterfly [13]. This link between the 2D HH and 1D AA models has also been explored from the point of view of topological properties [14–16]. This revealed connections with seemingly unrelated systems, such as topological insulators [17] and superconductors [18], as well as the quantum Hall effect (QHE) [19–21].

Lately, extensions of the AA model have been proposed [22,23] including periodic modulations of the nearest-neighbor hopping amplitude. An incommensurate hopping modulation leads to Anderson-like localization [22], thus mimicking disorder, as does the diagonal AA potential, while a commensurate modulation brings up new features, such as the appearance of zero-energy topological edge states [23]. Here we combine commensurate and incommensurate off-diagonal modulations, which turns out to be nontrivial from the point of view of topological properties. Indeed, we find that topological edge states are robust against an incommensurate perturbation, surviving the localization transition in a certain range of parameters. This result opens new perspectives for the investigation of the interplay between topology and disorder.

A generalized Aubry-André model, including commensurate and incommensurate hopping modulations as well as a diagonal incommensurate potential, may be described by the Hamiltonian

$$H = -t\sum_i[(1+\lambda_i+\delta_i)(a_{i+1}^\dagger a_i + \text{H.c.}) + \varepsilon_i a_i^\dagger a_i], \quad (1)$$

where

$$\lambda_i = \lambda\cos(2\pi bi+\varphi), \quad \delta_i = \delta\cos(2\pi\beta i+\varphi_\delta),$$
$$\varepsilon_i = \Delta\cos(2\pi\beta i+\varphi_\Delta) \quad (2)$$

are commensurate and incommensurate hopping modulations, and the diagonal AA potential, respectively; i assumes integer values labeling lattice sites; t represents the hopping (or tunneling) amplitude; the creation and annihilation operators $a_i^\dagger$ and a_i can be bosonic or fermionic (differences being in the nature of many-body states). The phases in the three periodic terms are possibly all different. The inverse wavelengths of commensurate and incommensurate modulations are respectively denoted as b and β. We will mostly focus on the case $b = 1/2$, and we fix $\beta = (1+\sqrt{5})/2$, the golden ratio. Without off-diagonal modulation ($\lambda = \delta = 0$), one recovers the usual AA model. For simplicity, we will refer to λ as *modulation amplitude*, and to Δ and δ as (respectively, diagonal and off-diagonal) *disorder strengths*, since the incommensurate terms can be viewed as a kind of (nonrandom) disorder.

Our aim is to investigate how the disorder perturbations affect the spectrum obtained in the commensurate case ($\Delta = \delta = 0$), with special attention to what happens to the topological states. We will do this by exact diagonalization on finite lattices. Complementing a direct visualization of the energy spectrum as it evolves under the perturbation, a more detailed analysis of its changes will be done by calculating the superfluid fraction [24], and the ground-sate *fidelity* [25]. This latter quantity is known to be a powerful tool to detect precursors of quantum phase transitions (QPTs). Particularly for the kind of lattice models addressed here, we have previously shown [9] that it is sensitive to ground-state changes at the QPT critical parameters even for fairly small systems.

II. LOCALIZATION

As mentioned above, an Anderson-like localization transition occurs in the usual AA model ($\lambda = \delta = 0$) for a critical $\Delta_c = 2t$ when β is the golden ratio. In a Bose-Einstein condensate, the localized phase is characterized by a null value of the superfluid fraction, which is calculated by imposing twisted periodic boundary conditions with a small twist angle θ. The superfluid fraction f_s is then proportional to the energy difference between twisted and nontwisted ground states divided by θ^2. For finite lattices, it is necessary to utilize a golden-ratio approximation as the quotient between

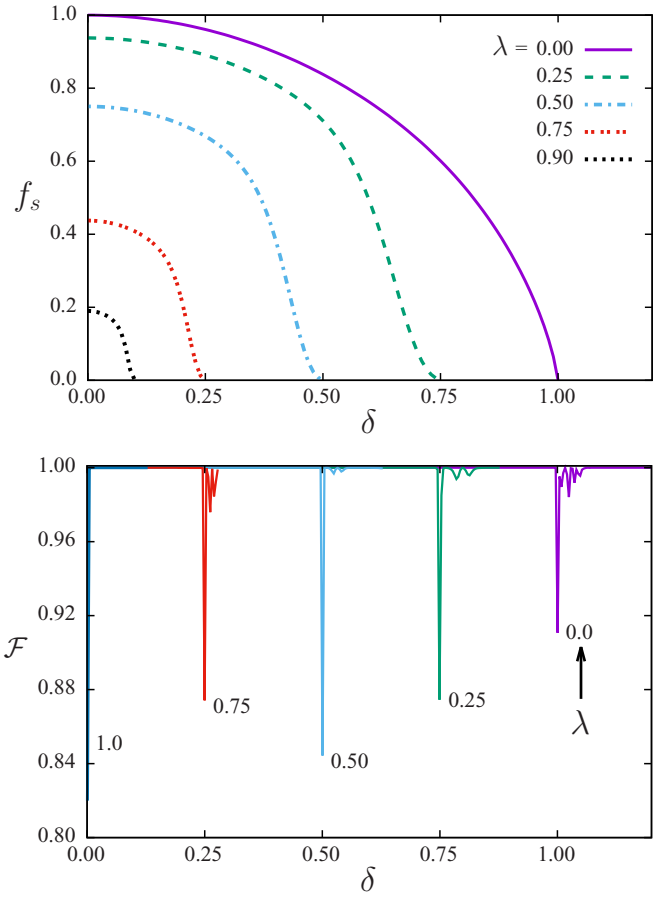

FIG. 1. Superfluid fraction (top) and ground-state fidelity (bottom) as functions of disorder strength δ for the indicated values of modulation amplitude λ. Notice the coincidence of critical points.

two consecutive Fibonacci numbers, one of which is the number of lattice sites [26]. On the other hand, the ground-state fidelity, in this case defined as the scalar product between two ground-state vectors corresponding to slightly different values of Δ, is able to detect the transition as a sharp minimum at Δ_c, both with periodic or open boundary conditions.

Anderson localization also occurs in generalized AA models with combined diagonal and off-diagonal disorder [22]. Here, we focus on purely off-diagonal disorder [$\Delta = 0, \delta \neq 0$ in Eqs. (1) and (2)] but in the presence of commensurate hopping modulation ($\lambda \neq 0$), in order to have zero-energy topological states. It turns out that the critical disorder strength δ_c depends on the modulation amplitude λ. The top panel of Fig. 1 shows the superfluid fraction f_s as a function of δ for $b = 1/2$ and different values of λ. One can clearly see critical values of δ at which f_s drops to zero, indicating localization. In the bottom panel of Fig. 1 we plot the fidelity between two ground-states differing by a small variation in δ. This fidelity has pronounced minima exactly at the values of δ for which the superfluid fraction vanishes, consistent with their identification as critical values for a localization transition.

The superfluid-fraction curves in Fig. 1 were obtained with periodic boundary conditions on lattices of 144 sites, with $\beta = 233/144$, a rational approximant of the golden ratio. On the other hand, fidelity values shown in the same figure were calculated with open boundary conditions for chains of 200 sites. The coincidence of δ_c values is remarkable. Other lattice sizes were checked with essentially coincident results.

A superfluid fraction in principle implies a bosonic system, while related problems, such as topological insulators and superconductors, involve fermions. However, the single-particle energy spectrum is the same, and our focus is on the noninteracting limit. A fundamental difference would be the relevance of the Fermi level rather than the lowest-energy state, but localization occurs for all states in one dimension. In practice, the superfluid fraction is used here only to indicate the presence of extended or localized states. It should also be noticed that f_s is proportional to the *helicity modulus* [27], which is more general, an can be viewed as a measure of wave-function coherence across the system.

The values of δ_c that we obtained obey a simple linear relation, $\delta_c(\lambda) = 1 - \lambda$. The maximum value of f_s is also strongly dependent on λ, as seen in Fig. 1. In particular, the curves $f_s(\delta)$ tend to a single point ($f_s = 0$, $\delta = 0$) for $\lambda = 1$. The kind of localization that occurs for $\lambda = 1$ when $\delta = 0$ can be understood as a cancellation of the uniform hopping term with the modulated one. Since $\cos(\pi i) = \pm 1$ for odd/even i, the net hopping amplitude $t(1 + \lambda_i)$ alternates between $2t$ and 0, so that the 1D lattice breaks down into isolated dimers, and the localization becomes *trivial*. If we then turn on the incommensurate hopping term, we find that the superfluid fraction remains zero, since this essentially random connection is not capable of building up extended states. All these results concerning localization were obtained for zero phases ($\varphi_\delta = \varphi = 0$). The effect of nonzero phases will be discussed in the following.

III. TOPOLOGICAL STATES

The purely commensurate off-diagonal model with $b = 1/2$ shows degenerate pairs of zero-energy topological states in the phase region $|\varphi| < \pi/2$ (and equivalent regions displaced by 2π) [23]. These states can be seen in the first plot of Fig. 2. Zero-energy topological states may be associated with Majorana fermions [18]. Such particles are their own antiparticles, i.e., creation and annihilation operators are equal. They can be defined as linear combinations of creation and annihilation operators for real fermions, which is possible in a particle-hole symmetric situation. Kitaev [28] used these operators in a simple mean-field model of a 1D superconductor with p-wave nearest-neighbor pairing. It defines a chain in which alternate pairs of sites are coupled, leaving two unpaired Majorana fermions at the ends. A real 1D superconductor, with spin-1/2 electrons, would not be time-reversal invariant in this case, and should belong to the topology class D [29]. However, the model as originally proposed, with spinless fermions, is both time-reversal invariant and particle-hole symmetric, which implies chiral (or sublattice) symmetry. So, the spinless Kitaev-model is classified into the BDI topology class [29]. This is the same topology of a tight-binding chain with alternating hopping integrals t_1,t_2, related to a model of polyacetylene [30]. It turns out to be also the topology of the purely commensurate generalized AA model with $b = 1/2$ in the phase region where topological states exist, where we have $t_1 = t(1 - \lambda\cos\varphi)$ and $t_2 = t(1 + \lambda\cos\varphi)$.

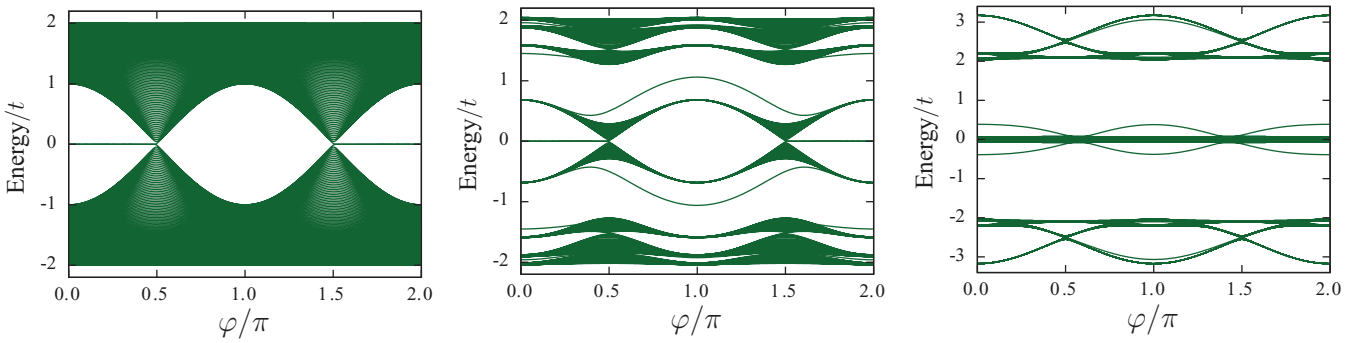

FIG. 2. Energy spectrum as a function of φ for $\lambda = 0.5$ and $\varphi_\delta = 0$, with $\delta = 0, 0.5, 1.5$ (from left to right). Gaps open up under the incommensurate perturbation, but eventually states are pushed to the low-energy region.

As implied by the above discussion, the observed topological states are *edge states*, hence only appearing for open boundary conditions. One should notice that, in contrast to what happens in the QHE, edge states in a 1D system are localized. Then, they may in principle survive after the system undergoes Anderson-like localization. We will show that it actually happens in the case off-diagonal disorder. In contrast, a diagonal AA potential displaces the edge states away from zero energy for any $\Delta \neq 0$, which is consistent with the breakdown of chiral symmetry by local disorder.

In Fig. 2 we plot the energy eigenvalues as functions of φ, for $\lambda = 0.5$ and fixed $\varphi_\delta = 0$, showing the trend of spectrum evolution as the disorder strength δ increases. Starting from the purely commensurate case (first plot), we observe that (*i*) gaps open up, and the bands are substantially reshaped when disorder is turned on (middle plot), but the topological states have not changed; (*ii*) at $\delta = 1.5$ (last plot), band states have been pushed to the middle of the gap, and the topological states are no longer visible. Thus, we find that the topological states survive the localization transition, but they eventually disappear at a new critical value $\bar{\delta}_c > \delta_c$. This is better seen in an expanded view of the low-energy region presented in Fig. 3. It highlights the states with energy close to zero near $\varphi = 0$, showing that in this case ($\lambda = 0.5$) the zero-energy degeneracy is lifted for $\bar{\delta}_c \simeq 1.5$, while at a slightly smaller value of δ the topological states are still clearly visible. The lower panels in Fig. 3 are plots of wave-function amplitudes corresponding to the indicated eigenvalues. At $\bar{\delta}_c$ the states no longer have the edge character still noticeable for $\delta = 1.49$.

As observed for δ_c in the localization transition, the critical value $\bar{\delta}_c$ also varies with λ. Systematically studying this variation, we found that it also follows a simple linear relationship, which in this case is $\bar{\delta}_c = 1 + \lambda$. Based on this, we constructed a phase diagram of the generalized AA model (without site-diagonal potential), shown in Fig. 4. It presents three distinct phases: conductor with Majorana states (I), Anderson insulator with Majorana states (II), and Anderson insulator without Majorana states (III). By *conductor* we mean a system in which the bulk single-particle states are extended.

The phase diagram of Fig. 4 is for null phases ($\varphi_\delta = \varphi = 0$). The role of φ is easily revealed. As we are restricting ourselves to the $b = 1/2$ model, the λ_i term in (1) is, in fact, $\lambda\cos(\pi i + \varphi) = \lambda\cos(\varphi)\cos(\pi i) = \lambda\cos(\varphi)\cos(2\pi b i)$. Therefore, the results for $\varphi \neq 0$ can be directly obtained from the ones for $\varphi = 0$ by just substituting $\lambda_\varphi \equiv \lambda\cos(\varphi)$ for λ. Then, to obtain phase diagrams for nonzero values of φ it suffices to rescale the horizontal axis in Fig. 4 by a factor $1/\cos(\varphi)$. With this, the value of λ for which δ_c vanishes moves to the right, and the angle between the two straight lines decreases. When $\varphi = \pi/2$, the point $\lambda_\varphi = 1$ corresponds to $\lambda \to \infty$, and the two lines coincide horizontally, implying that the only transition occurs at $\delta_c = 1$, between a conductor and an Anderson insulator. This happens at the "Dirac points" of the purely commensurate spectrum (first plot in Fig. 2) for which we have a single continuous band and no topological states. For any finite λ, this is equivalent to a simple lattice (uniform nearest-neighbor hopping), to which addition of an incommensurate hopping modulation leads to localization at $\delta = 1$.

The effect of varying the phase φ_δ of the disorder term is not as easy to describe in a general way since it is not possible to absorb this phase into an effective amplitude. So

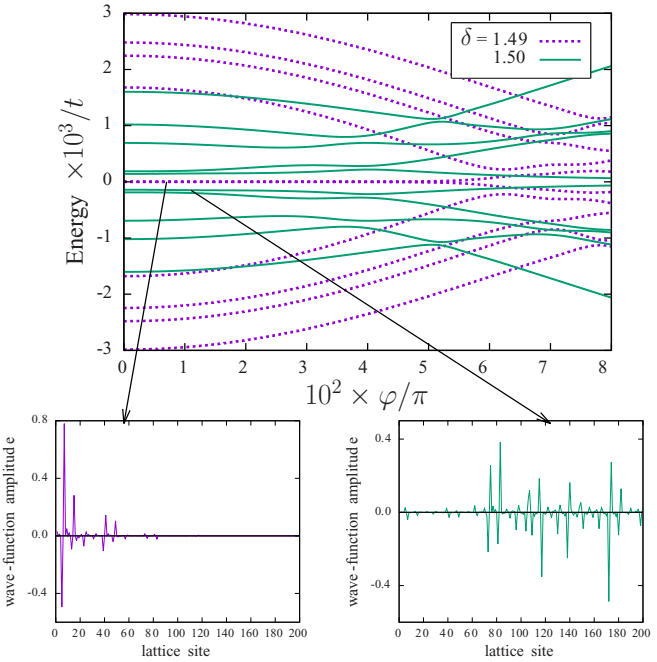

FIG. 3. Expanded view (notice the scale factors) of the spectra for $\lambda = 0.5$ and two values of δ around the critical value for which topological states are suppressed. Representative wave functions (lower plots) show the edge character of zero-energy states (left), absent when they split off (right).

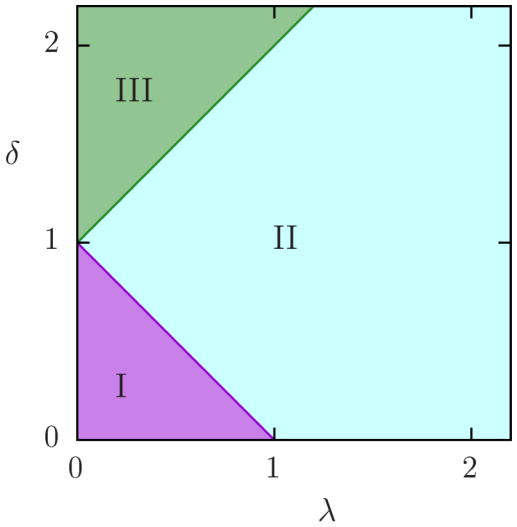

FIG. 4. Phase diagram of model (1) with $\Delta = 0$. The phases are (I) conductor with Majorana states, (II) Anderson insulator with Majorana states, and (III) Anderson insulator without Majorana states.

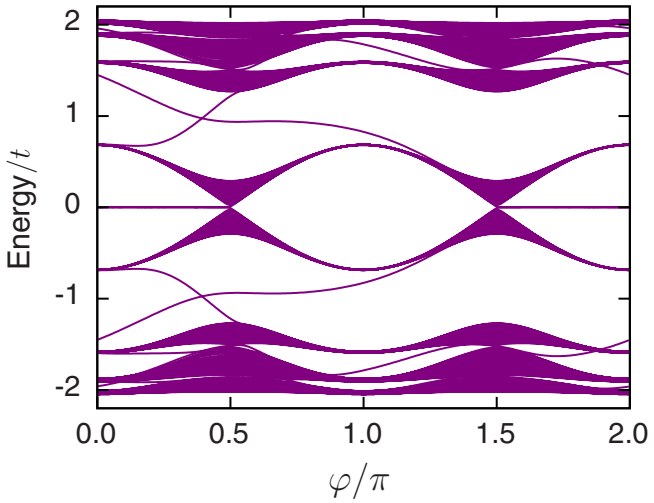

FIG. 5. Energy spectrum of the generalized AA model with locked modulation phases $\varphi_\delta = \varphi$. In this example we have $\lambda = \delta = 0.5$. Notice that pairs of edge states connect neighboring bands across the gaps. Otherwise, the spectrum is very similar to the one for $\varphi_\delta = 0$ shown in Fig. 2.

far our analysis has been restricted to $\varphi_\delta = 0$. If we now lock the phases of commensurate and incommensurate modulations ($\varphi_\delta = \varphi$), the overall spectrum structure remains essentially as in Fig. 2, except for one important difference: the bands never truly split off with increasing δ, but remain connected across the gaps by pairs of edge states. These are reminiscent of edge states in topological insulators or the QHE. However, Majorana states are also present in the region of small $|\varphi_\delta|$ (mod 2π). An example spectrum is presented in Fig. 5. The low-energy region near $\varphi = 0$ in the coupled-phases model is very similar to that presented in Fig. 3, indicating that the survival and subsequent disappearance of zero-energy states is not significantly changed by phase locking in that region. However, we have preliminary evidence that zero-energy states may continue to exist for other phase values. This interesting possibility deserves further investigation.

The observed spectral differences indicate that the generalized off-diagonal AA model with coupled phases and the one with the incommensurate-term phase fixed at zero belong to different topological classes. The model with coupled phases has the same topology as the purely commensurate one ($\lambda \neq 0, \delta = 0$), since one spectrum can be "deformed" into the other, by variation of the parameter δ, without closing (or opening) gaps. This is not the case with fixed $\varphi_\delta = 0$, as shown in Fig. 2. The existence of different topologies can be understood by the effective two-dimensionality of the AA model in its correspondence to the HH model, as discussed in the Introduction. In fact, the phase φ is actually a degree of freedom since it is proportional to the transverse momentum of the electrons in the 2D model.

IV. CONCLUSIONS

We investigated extensions of the one-dimensional Aubry-André model in which a commensurate modulation of the hopping amplitude gives rise to topological states of zero energy, associated with Majorana fermions. We focused on how an off-diagonal disorder, realized by an incommensurate hopping modulation, affects the energy spectrum, inducing Anderson-like localization. We found out that the topological zero-energy states survive after the localization transition up to a second critical value of the disorder strength. In addition, we observed that topological properties depend on the relationship between the phases of commensurate and incommensurate modulations.

Real physical systems, ranging from polymers [30] and solid-state nanostructures [28] to optically confined cold-atom lattices [1,2,31] and light propagation in waveguide arrays [3,15], can be described by the kind of models studied here. The fact that quasiperiodic potentials can be realized in these systems implies that experimental investigations of the interplay between topology and disorder that we addressed here can be carried on.

ACKNOWLEDGMENT

We acknowledge support from the Brazilian agency Conselho Nacional de Desenvolvimento Científico e Tecnológico.

[1] J. Billy, V. Josse, Z. Zuo, A. Bernard, B. Hambrecht, P. Lugan, D. Clément, L. Sanchez-Palencia, P. Bouyer, and A. Aspect, Nature (London) **453**, 891 (2008).

[2] G. Roati, C. D'Errico, L. Fallani, M. Fattori, C. Fort, M. Zaccanti, G. Modugno, M. Modugno, and M. Inguscio, Nature (London) **453**, 895 (2008).

[3] Y. Lahini, R. Pugatch, F. Pozzi, M. Sorel, R. Morandotti, N. Davidson, and Y. Silberberg, Phys. Rev. Lett. **103**, 013901 (2009).
[4] P. W. Anderson, Phys. Rev. **109**, 1492 (1958).
[5] S. Das Sarma, S. He, and X. C. Xie, Phys. Rev. Lett. **61**, 2144 (1988).
[6] S. Das Sarma, S. He, and X. C. Xie, Phys. Rev. B **41**, 5544 (1990).
[7] J. Biddle, B. Wang, D. J. Priour, and S. Das Sarma, Phys. Rev. A **80**, 021603 (2009).
[8] J. Biddle and S. Das Sarma, Phys. Rev. Lett. **104**, 070601 (2010).
[9] J. C. C. Cestari, A. Foerster, and M. A. Gusmão, Phys. Rev. A **82**, 063634 (2010).
[10] J. C. C. Cestari, A. Foerster, M. A. Gusmão, and M. Continentino, Phys. Rev. A **84**, 055601 (2011).
[11] S. Aubry and G. André, Ann. Israel Phys. Soc. **3**, 133 (1980).
[12] P. G. Harper, Proc. Phys. Soc. London, Sect. A **68**, 874 (1955).
[13] D. R. Hofstadter, Phys. Rev. B **14**, 2239 (1976).
[14] L.-J. Lang, X. Cai, and S. Chen, Phys. Rev. Lett. **108**, 220401 (2012).
[15] Y. E. Kraus, Y. Lahini, Z. Ringel, M. Verbin, and O. Zilberberg, Phys. Rev. Lett. **109**, 106402 (2012).
[16] Y. E. Kraus and O. Zilberberg, Phys. Rev. Lett. **109**, 116404 (2012).
[17] M. Z. Hasan and C. L. Kane, Rev. Mod. Phys. **82**, 3045 (2010).
[18] M. Leijnse and K. Flensberg, Semicond. Sci. Technol. **27**, 124003 (2012).
[19] R. B. Laughlin, Phys. Rev. B **23**, 5632 (1981).
[20] D. J. Thouless, M. Kohmoto, M. P. Nightingale, and M. den Nijs, Phys. Rev. Lett. **49**, 405 (1982).
[21] Y. Hatsugai, Phys. Rev. Lett. **71**, 3697 (1993).
[22] F. Liu, S. Ghosh, and Y. D. Chong, Phys. Rev. B **91**, 014108 (2015).
[23] S. Ganeshan, K. Sun, and S. Das Sarma, Phys. Rev. Lett. **110**, 180403 (2013).
[24] R. Roth and K. Burnett, Phys. Rev. A **68**, 023604 (2003).
[25] M. A. Nielsen and I. L. Chuang, *Quantum Computation and Quantum Information* (Cambridge University Press, Cambridge, 2000).
[26] M. Kohmoto, Phys. Rev. Lett. **51**, 1198 (1983).
[27] M. E. Fisher, M. N. Barber, and D. Jasnow, Phys. Rev. A **8**, 1111 (1973).
[28] A. Y. Kitaev, Phys. Usp. **44**, 131 (2001).
[29] A. P. Schnyder, S. Ryu, A. Furusaki, and A. W. W. Ludwig, Phys. Rev. B **78**, 195125 (2008).
[30] W. P. Su, J. R. Schrieffer, and A. J. Heeger, Phys. Rev. Lett. **42**, 1698 (1979).
[31] S. Nakajima, T. Tomita, S. Taie, T. Ichinose, H. Ozawa, L. Wang, M. Troyer, and Y. Takahashi, Nat. Phys. **12**, 296 (2016).